

# Chapter 19

## Analysis of Fiber Laser Micro-grooving on 316 L Stainless Steel



A. Sen , B. Doloi  and B. Bhattacharyya

**Abstract** Within the domain of austenitic stainless steel, 316 L stainless steel is widely used in both biomedical and automotive industries due to its superior mechanical properties. In the present research study, the performance of the fiber laser micro-grooving process with regard to kerf width and surface roughness  $R_a$  has been analyzed. The process parameters, i.e., laser power (7.5–20 W), pulse frequency (55–80 kHz), and cutting speed (0.5–3 mm/s) are considered to examine the aforesaid responses. The results of the experiments exhibit that the presence of flowing condition of the high-pressure assist air in combination with varying aforesaid process parameters, have a considerable effect on the kerf width characteristics along with the average surface roughness  $R_a$  of microgroove cut on 316 L stainless steel.

**Keywords** Fiber laser · Micro-grooving · Stainless steel · Kerf width · Surface roughness

### 19.1 Introduction

Over the past decade, it has been observed that fiber lasers have played an essential role in the laser industries ranging from high to low power laser sources required for various engineering applications. Although the number of research works utilizing fiber lasers has increased in the previous years, the research works integrating fiber lasers have not yet obtained their optimum utilization in the domain of micromachining. At present, the utilization of fiber laser micromachining process on 316 L stainless steel (SS) for the manufacturing of stents has increased rapidly. The previous research works involving 316 L showcase various aspects of geometrical features such as kerf width, depth in order to achieve desired profiles, etc.

A pulsed fiber laser setup was utilized by Meng et al. [1] in order to fabricate stents on 316 L. Laser output power, pulse frequency, pulse length, assist gas pressure (oxygen) along with cutting speed were considered as the primary process parameters for

---

A. Sen (✉) · B. Doloi · B. Bhattacharyya  
Production Engineering Department, Jadavpur University, Kolkata 700032, India  
e-mail: [abhishek.sen1986@gmail.com](mailto:abhishek.sen1986@gmail.com)

the analysis of the kerf width. With the change in laser power along with the cutting speed, the kerf width dimensions were varied significantly. The authors found that at a laser power 7 W, 0.15 ms pulse duration, cutting speed of 8 mm/s, assist oxygen pressure of 0.3 MPa, and pulse frequency of 1500 Hz, the kerf width along with surface roughness and heat-affected zone (HAZ) width was minimized. A comparative study of fiber laser micro-cutting on 316 L under different conditions was performed by Muhammed et al. [2]. The authors derived that, in the wet condition, kerf width was low in comparison to that of the dry condition. The back wall damages along with HAZ width were reduced significantly during the wet condition. Kleine et al. [3] further utilized single-mode fiber laser in order to micro-cut stainless steel stents. The considered responses were kerf width and surface quality on the sidewall of the micro-cut profiles. The authors concluded that during high settings of pulse frequency, spot overlap was a dominant factor which in turn produced low and good quality kerf widths. However, when the spot overlap reached over 85%, the factor was insignificant for surface roughness parameters. Sen et al. [4] on the other hand, carried out a fiber laser micro-grooving operation on 316 L SS at 200, 250 °C as well as at room temperature to assess the influence of cutting speed and laser beam focal position on the kerf width in combination with HAZ width. The authors also found out that at 250 °C, the uniformity of the micro-groove profiles was higher compared to the other temperatures. However, at room temperature, kerf width along with the HAZ width dimension was relatively lower compared to the elevated temperatures. Further, the uniformity and waviness of the profiles were also affected considerably in the room temperature compared to the higher temperatures. The authors concluded that the formation of taper notably affected the uniformity as well as the kerf width of the micro-groove profiles. Fuss et al. [5] showcased that when micro-grooves were generated on the surface of 316 L, the rate of human aortic endothelial cells (HAEC) increased significantly. Thus, it is essential to fabricate micro-grooves on 316 L in order to utilize the stent with its specific geometrical features to improve the biocompatibility as well as the tissue response time.

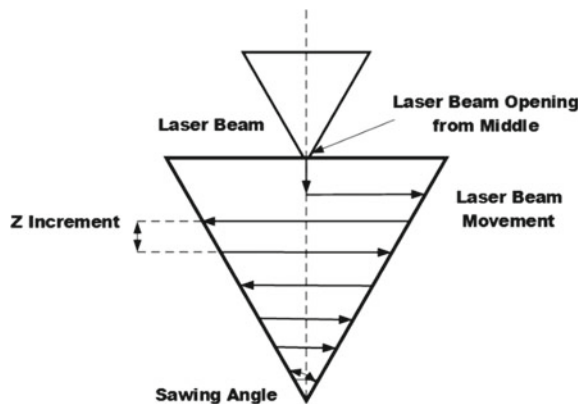
In this regard, the assessment of fiber laser on the machinability of 316 L SS (at room temperature) in atmospheric condition and in flowing assist air condition is yet to be carried out by the researchers. The high range of pulse frequency which leads to an increment in the laser spot overlapping factor has also not been studied extensively. From the trial runs, the selection of process parameters is carried out for the present study. Further, laser beam sawing angle, along with the laser beam opening type (the offset value between the micro-groove cut width and micro-groove wall), is correlated to the surface profiles of the fiber laser fabricated micro-grooves with the considered process parameters to study their effects on the performance criteria.

In this present research study, a comparative analysis has been conducted in order to find out the effect of fiber laser process parameters, i.e., cutting speed, laser power, and pulse frequency in atmospheric condition as well as in condition of flowing assist air pressure on kerf width and surface roughness  $R_a$  of micro-groove cut on 316 L SS by fiber laser micromachining process.

## 19.2 Experimental Plan

In the present research study, a total of 18 experiments has been carried out on 316 L SS (50 mm × 50 mm × 1 mm) without the supply of assist air, i.e., in atmospheric condition. In addition to this, with a similar set of process parameters, the same number of experiments is repeated with assist airflow at a pressure of 4 kgf/cm<sup>2</sup>. In each set of experiment, one process parameter is kept as a variable while the remaining two process parameters are kept as constants at their lowest values, considered in the experimental investigation. A total of 36 experiments is carried out with multi-diodes pumped 50 W nanosecond pulsed fiber laser system. However, in the present research work, due to the Gaussian beam profile of the laser beam, straight cut micro-groove profiles have been fabricated with the triangle-shaped formation at the depth edges. The experiments are categorized into three sets in which one set of the process parameter is varied with and without the supply of high-pressure assist air. The experiments are carried out by utilizing software designed for micro-cutting applications, in which the offset value (based on the sawing angle) between the micro-groove width and micro-groove wall in combination with the sawing angle has a notable influence. The higher the sawing angle, the higher is the opening of the micro-groove profile. Thus, in order to achieve smaller dimensions of kerf width, a low sawing angle is preferred. As a result, in the present research study, the sawing angle is made constant at 0.01°. In Fig. 19.1, a schematic diagram comprising the movement of the laser beam inside a micro-groove is exhibited. The micro-groove profiles are measured by Leica optical microscope at 1.25×, 20× and 50× optical lenses. The surface roughness ( $R_a$ ) is measured by a Mitutoyo SJ 410 surface roughness tester with a Gaussian filter. Parameters related to surface roughness measurements are as follows: sampling length ( $l$ ) of 4 mm and cut-off length ( $\lambda_c$ ) of 0.8. The measurements of both the kerf width and surface roughness are carried out at five reference lines, and the result is the average of these values. The array of fiber laser fabricated micro-grooves is shown in Fig. 19.2.

**Fig. 19.1** Schematic diagram of laser beam movement during micro-groove formation



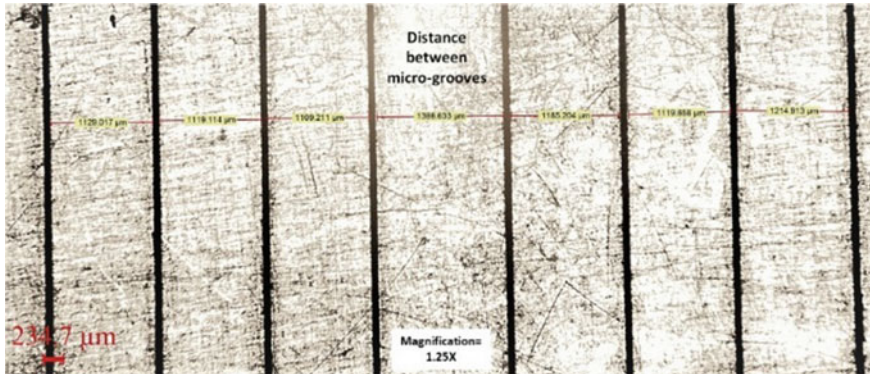


Fig. 19.2 Microscopic view of an array of fiber laser fabricated micro-grooves

### 19.3 Experimental Results

A total of 18 experiments (corresponds to three sets of experiments) has been performed without assist air along with another 18 experiments, which have been repeated with the aid of high-pressure assist air. The effect of laser power, pulse frequency, and cutting speed with respect to surface roughness parameters of fiber laser produced micro-grooves on 316 L SS are discussed and analyzed subsequently.

#### 19.3.1 Effect of Laser Power on Kerf Width and Surface Roughness, $R_a$

In the first set of experiments, the laser power is varied from 7.5 to 20 W while the other fixed parameters are set at a pulse frequency of 55 kHz, cutting speed of 0.5 mm/s and the duty cycle of 99%. The high value of the duty cycle is considered for all the 36 experiments in order to achieve high laser power corresponding to the input laser power value. Figure 19.3 corresponds to the effect of laser power on kerf width during the supply of assist air and without the assist air supply. Figure 19.4 represents the effect of laser power on surface roughness  $R_a$  with and without the supply of high-pressure assist air. The average value of  $R_a$  to assist air supply and without assist air is found at 2.13  $\mu\text{m}$  and 2.09  $\mu\text{m}$ , respectively.

In Fig. 19.3, it can be observed that in the presence of assist air supply, the kerf width dimensions tend to increase more compared to the experiments conducted without the supply of assist air. However, the maximum kerf width dimension is found to be 97.44  $\mu\text{m}$  in the absence of assist air at a laser power of 20 W. Advancement of high laser power causes high laser peak power in the machining zone. Subsequently, a high amount of energy is further generated by an increase in the laser peak power. Therefore, immediate melting and vaporization occur in the machined

**Fig. 19.3** Effect of laser power on kerf width

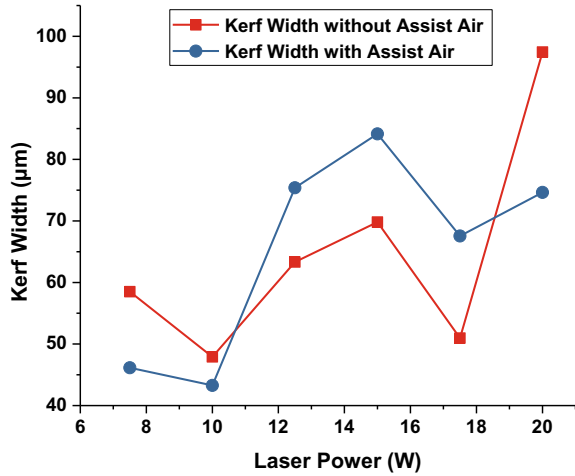
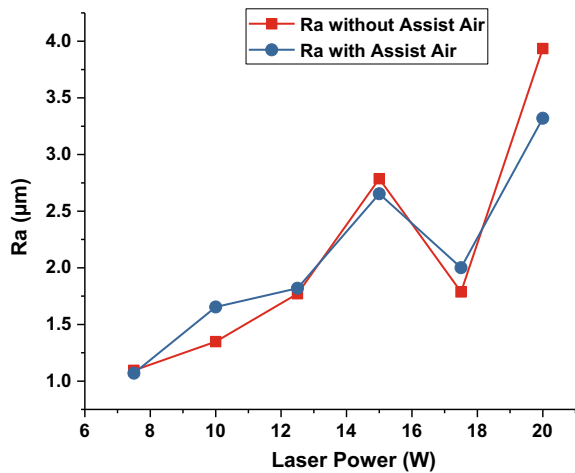


**Fig. 19.4** Effect of laser power on  $R_a$



zone subsequently. Furthermore, a high amount of material is removed and leads to high kerf width dimensions. The presence of a high-pressure flow of assist air has attributed less formation of resolidified material at the micro-groove edges which in turn has increased the kerf width dimensions. However, when the laser power reaches 20 W, sufficient amount of laser pulse energy, as well as laser beam peak power, can remove the resolidified material from the edges and lead to a steep rise in the kerf width dimension.

From Fig. 19.4, it is noted that when laser power increases up to 15 W,  $R_a$  tends to increase irrespective of the supply of assist air. A drop in values of  $R_a$  can be observed at a laser power of 17.5 W in which the high flow of assist air aids in lowering of  $R_a$  value considerably. This phenomenon can be the effect of resolidified material

along the micro-groove zone which lowers the surface roughness. Furthermore, with the increment in laser power, there is a rapid increase in  $R_a$  value in both the conditions due to the reason that the machining zone gets the suitable energy to melt and evaporate instantly. Thus, the laser peak power intensity can penetrate furthermore. However, simultaneous evaporation of the surfaces may occur in the irradiated spot center, and therefore, the irradiated laser surface shows a bumpy surface. The high amount of removal of material is observed during the flow of high pressurized assist air while combining with high laser power. It is also observed that the homogeneity of the micro-groove profiles is inconsistent throughout the entire length of the micro-groove.

### 19.3.2 Effect of Pulse Frequency on Kerf Width and Surface Roughness, $R_a$

In the second set of experiments, pulse frequency varies from 55 to 80 kHz, whereas the constant parameters are laser power of 7.5 W, cutting speed of 0.5 mm/s with and without the supply of assist air. Figure 19.5 shows the effect of pulse frequency on kerf width with and without the supply of assist air whereas the effect of pulse frequency on surface roughness  $R_a$  is shown in Fig. 19.6. The effect of the supply of high-pressure assist air with the increment of pulse frequency is found to be more predominant than the laser power. From Fig. 19.5, it is observed that in the presence of assist air supply, kerf width dimensions are reduced with the high values of pulse frequency. On the contrary, a reverse phenomenon is observed with the absence of assist air. During pulse frequency of 75 and 80 kHz, a notable decrease in the values of kerf width dimensions is observed in the presence of assist air supply, although the

**Fig. 19.5** Effect of pulse frequency on kerf width

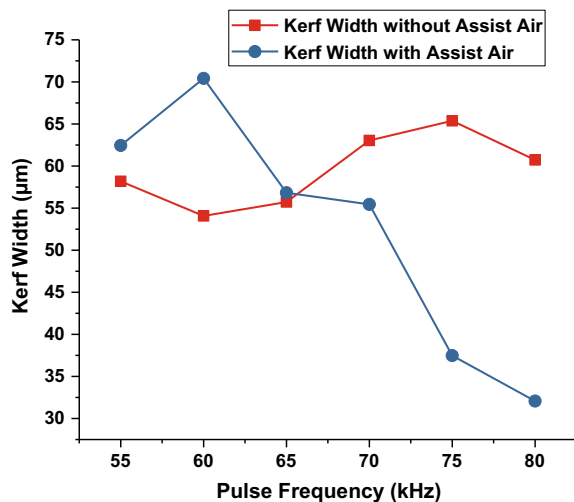
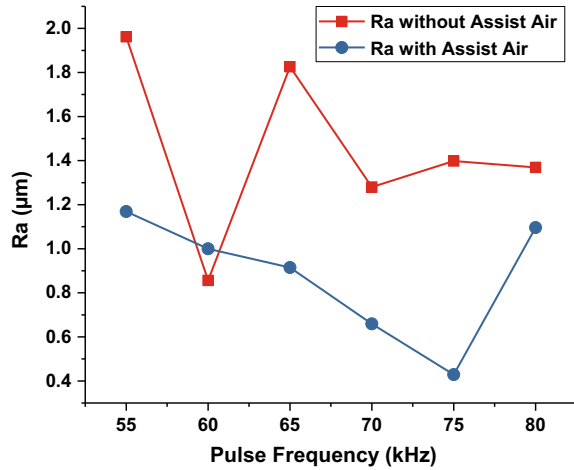


**Fig. 19.6** Effect of pulse frequency on  $R_a$



drop in laser peak power is inevitable at a high pulse frequency setting. A high number of laser pulses induce high laser material interaction time while keeping the pulse energy constant. In the absence of assist air supply, high laser material interaction time provides a sufficient amount of time for the ablation of material removal. The resolidification phenomenon along with HAZ are the dominant factors in absence of assist air. Resolidification phenomenon reverses and leads to the lowering of kerf width dimensions due to high spot overlapping factor in combination with the flow of high-pressure assist air. In addition to this, the changes in kerf width dimensions without assist air are not as high as compared to the assist air supply. High-pressure assist air forces the extra amount of molten material from the machining zone, leading to the reduction in kerf width dimension along with the thicker cut width.

When pulsed laser beam irradiates on 316 L SS surface, a thin melted layer is formed on the machined surface. Further, the machined surface is found to be less interrupted by the liquid displacement on the micro-machined zone. This phenomenon is due to the action of recoil pressure [6], formed during the fiber laser interaction with 316 L surface. As a result, smooth machined surfaces can be observed at a high pulse frequency. The effect is prominent when a high jet flow of assist air is applied to remove the molten material from the micro-groove zone. As the material removal rate is low at high pulse frequency due to low laser beam peak power, the flow of high-pressure assist air reduces the attributes of sputtering as well as HAZ width from the micro-groove profiles. The absence of assist air supply leads to high values of  $R_a$  in comparison to the presence of assist air supply. Thus, high peak power in combination with assist air significantly reduces  $R_a$  in a considerable amount. Only when the pulse frequency is kept as 80 kHz in the presence of assist air supply,  $R_a$  tends to showcase an observable rise as compared to the previous set of values.

At 50 $\times$  magnification, a microscopic view of the micro-grooves profiles cut at the variation of pulse frequency in the presence of assist air supply has been shown

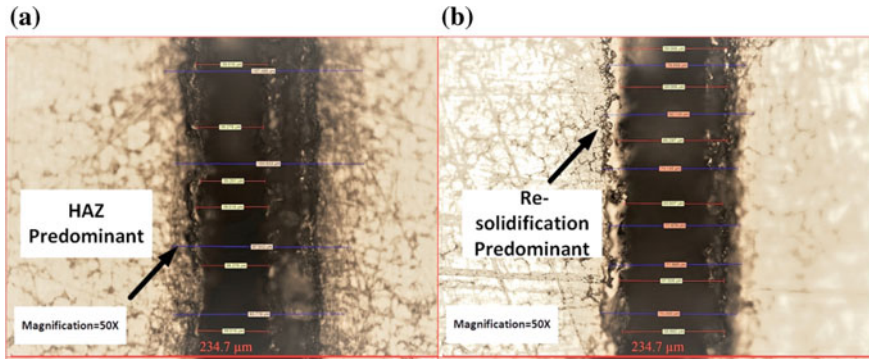


**Fig. 19.7** **a** Microscopic view of a micro-groove profile at 50× magnification at a pulse frequency of 80 kHz. **b** Microscopic view of micro-groove profile at 70 kHz of pulse frequency during assist air pressure (constants: laser power of 7.5 W and cutting speed of 0.5 mm/s)

in Fig. 19.7. From Fig. 19.7a, b, it is evident that HAZ is a detrimental factor which hinders while obtaining a uniform and smooth micro-groove profile.

### 19.3.3 Effect of Cutting Speed on Kerf Width and Surface Roughness, $R_a$

In this set of experiments, pulse frequency of 80 kHz and laser power of 7.5 W are kept as constants. The effects of cutting speed with and without assist air supply on kerf width are shown in Fig. 19.8. Figure 19.9 depicts the effect of cutting speed on average surface roughness  $R_a$  of the cut surface of micro-groove with and without assist air supply. The supply of high-pressure assist air has considerably improved micro-groove homogeneity by reducing the surface roughness. At higher cutting speed, kerf width without assist air follows a gradual decrease in the kerf width dimension as observed from Fig. 19.8.

On the contrary, a kerf width dimension in the presence of assist air is higher at cutting speed of 1.5 mm/s, followed by a gradual decrease in the kerf width dimensions. The average dimensions of the kerf width are comparatively higher when the assist air is supplied at high pressure. This increment in kerf width dimension suggests that assist air supply has partially blown away the molten material from the machining zone to facilitate more penetration of the laser beam in the machining zone. Machining time in combination with the assist air determines the homogeneity and uniformity of the micro-groove profiles. When the cutting speed increases, it is evident that the machining time is subsequently reduced, which in turn lowers the kerf width dimensions. When the laser beam moves to and fro with the machining zone as shown in Fig. 19.1, some amount of molten material is accumulated at the machining zone which ultimately reduces the laser beam penetration rate. At



**Fig. 19.8** Effect of cutting speed on kerf width

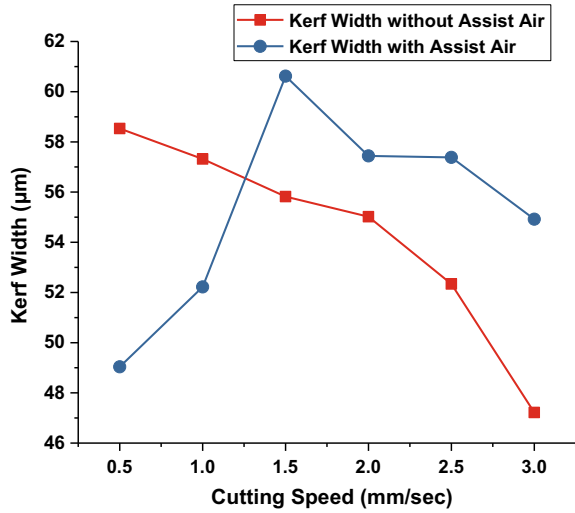
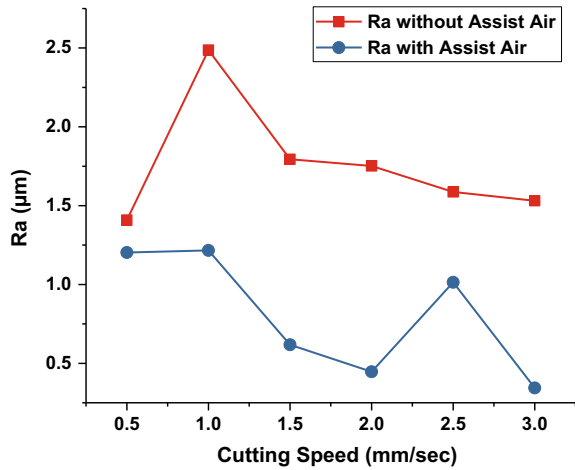


**Fig. 19.9** Effect of cutting speed on  $R_a$



each pass, the penetration rate is decreased with or without the supply of assist air. However, a sufficient amount of assist air pressure leads to the removal of the molten material and subsequently increases the kerf width dimensions. This increment in kerf width dimensions holds true at higher assist air pressure in combination with cutting speed of 1.5 mm/s. Nevertheless, low machining time along with low penetration rate ultimately reduces the kerf width dimension as observed from Fig. 19.8.

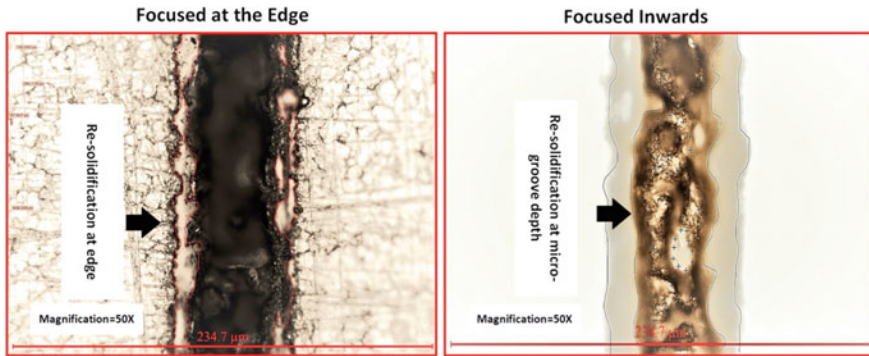


**Fig. 19.10** Microscopic view of fiber laser fabricated micro-groove profiles at 50× magnification

Selection of cutting speed along with pulse frequency determines the laser spot overlapping factor and laser–material interaction time. The lower laser material interaction time during high cutting speed helps to reduce the surface roughness parameters considerably. When high cutting speed (low MRR) in combination with high-pressure assist air comes into effect, the excess amount of molten material is blown away [7]. In the presence of assist air, heat can quickly go out from the machining zone. This loss of energy successively produces resolidified material on the inner surfaces of the micro-grooves as shown in Fig. 19.10. Without the supply of assist air, it is difficult to remove the extra amount of molten material from the micro-groove periphery. Furthermore, in the absence of assist air, the excess amount cannot be blown away completely which results in high surface roughness,  $R_a$ .

## 19.4 Conclusions

Fiber laser micro-grooving of 316 L SS has been studied to analyze the effect of the flow of high-pressure assist air on micro-groove kerf width and average surface roughness  $R_a$ . In the presence of assist air supply at high laser power, the kerf width dimensions tend to increase more rapidly as compared to the experiments conducted without assist air supply. The effect of assist air supply is more on the kerf width dimensions in combination with high values of pulse frequency. Without the presence of assist air, the kerf width dimensions tend to increase with the increase in pulse frequency, whereas the reverse phenomenon is observed with the aid of assist air. At cutting speed of 1.5 mm/s, the presence of the jet of assist air results in a larger kerf width of micro-groove. Higher ranges of kerf width dimensions are observed when the assist air is supplied during the fiber laser micro-grooving on 316 L SS.

The experimental results also indicate that the effect of assist air is prominent in order to achieve a low average surface roughness of the cut profiles. In the presence of high-pressure assist air, the average surface roughness  $R_a$  of the cut profiles increases

with the increment of laser power. The similar phenomenon is also observed in the experiments conducted without the presence of assist air supply. However, it is observed that the difference in the obtained surface roughness values in both the cases does not exhibit observable differences. Due to the supply of high-pressure assist air, surface roughness values decrease for high values of pulse frequency. An opposite set of the phenomenon is observed in the experiments conducted without the supply of assist air. At higher cutting speed in the presence of a jet flow of assist air supply, surface roughness values lower at a considerable amount as compared to the experiments conducted without the supply of assist air.

The research findings are useful in order to analyze other surface characteristics such as waviness, tapering of the micro-grooves, and also to obtain the desired micro-groove geometries with respect to the considered process parameters during fiber laser micro-grooving on 316 L stainless steel.

**Acknowledgements** The authors would like to express their gratitude toward the assistance and financial support aided by CAS Ph-IV Programme of the Production Engineering Department of Jadavpur University under the University Grants Commission, New Delhi, India.

## References

1. Meng, H., Liao, J., Zhou, Y., Zhang, Q.: Laser micro-processing of cardiovascular stent with fiber laser cutting system. *Opt. Laser Technol.* **41**(3), 300–302 (2009). <https://doi.org/10.1016/j.optlastec.2008.06.001>
2. Muhammad, N., Whitehead, D., Boor, A., Li, L.: Comparison of dry and wet fibre laser profile cutting of thin 316 L stainless steel tubes for medical device applications. *J. Mater. Process. Technol.* **210**(15), 2261–2267 (2010). <https://doi.org/10.1016/j.jmatprotec.2010.08.015>
3. Kleine, K.F., Whitney, B., Watkins, K. G.: Use of fiber lasers for micro cutting applications in the medical device industry. *International Congress on Applications of Lasers & Electro-Optics* (2002)
4. Sen, A., Doloi, B., Bhattacharyya, B.: Fiber laser micro-grooving of 316 L stainless steel utilizing variable temperature heating apparatus. In: *Proceedings of the All India Manufacturing Technology Design and Research Conference*, Pune, India, pp. 285–289 (2016)
5. Fuss, C., Sprague, E.A., Bailey, S.R., Palmaz, J.C.: Surface micro grooves (MG) improve endothelialization rate in vitro and in vivo. *J. Am. Coll. Cardiol.* **37**(2), 70A–70A (2001)
6. Soveja, A., Cicală, E., Grevey, D., Jouvard, J.M.: Optimization of TA6V alloy surface laser texturing using an experimental design approach. *Opt. Lasers Eng.* **46**(9), 671–678 (2008). <https://doi.org/10.1016/j.optlaseng.2008.04.009>
7. El Aoud, B., Boujelbene, M., Bayraktar, E., Salem, S.B., Miskioglu, I.: Studying effect of CO<sub>2</sub> laser cutting parameters of titanium alloy on heat affected zone and kerf width using the Taguchi method. In: *Mechanics of Composite and Multi-functional Materials*, 6th edn. Springer, Cham (2018). [https://doi.org/10.1007/978-3-319-63408-1\\_14](https://doi.org/10.1007/978-3-319-63408-1_14)